# Measurement of the short-time self-mobility of particles in concentrated suspension. Evidence for many-particle hydrodynamic interactions

P.N. Pusey, W. van Megen

LE JOURNAL DE PHYSIQUE

*J. Physique* **44** (1983) 285-291 MARS **1983,** PAGE 285

Classification
*Physics Abstracts*
05.40 — 82.70

# Measurement of the short-time self-mobility of particles in concentrated suspension. Evidence for many-particle hydrodynamic interactions

P. N. Pusey

Royal Signals and Radar Establishment, Malvern, Worcestershire, WR14 3PS, England

and W. van Megen

Department of Applied Physics, Royal Melbourne Institute of Technology, Melbourne, Victoria, Australia

(*Reçu le 27 juillet 1982, accepté le 25 novembre 1982*)

**Résumé.** — Nous avons mesuré par spectroscopie de corrélation de photons la self-mobilité aux temps courts de particules colloïdales sphériques dans des suspensions liquides concentrées. Pour des fractions en volume $\phi \gtrsim 0{,}3$, la théorie incluant les interactions hydrodynamiques à deux corps ne permet pas de décrire nos résultats, ce qui indique l'importance des interactions multiples.

**Abstract.** — The short-time self-mobilities of spherical colloidal particles in concentrated liquid suspensions were measured by photon correlation spectroscopy. For volume fractions $\phi \gtrsim 0.3$, theory incorporating two-particle hydrodynamic interactions was not adequate to describe the data, indicating the importance of many-particle contributions.

1. **Introduction.** — Concentrated suspensions of microscopic particles in a liquid occur widely in nature and are of importance in many industrial processes. In fairly dilute suspensions (volume fraction $\phi < 0.05$, say) the effects on particle Brownian motions of both direct interparticle interactions (for example, coulombic or « hard-sphere ») and indirect hydrodynamic interactions (transmitted through fluctuating flows in the suspending liquid) are reasonably well understood theoretically [1-7]. At these concentrations it is adequate to treat hydrodynamic interactions as pairwise additive. However, at larger $\phi$, clusters of more than two particles become probable and the validity of assuming pairwise additivity of hydrodynamic interactions is questionable. Here we report measurements by photon correlation spectroscopy of the mobility, over distances small compared to the particle radius, of single particles in suspensions of volume fractions up to about 0.45. This local self-mobility is possibly the simplest useful dynamic property of a concentrated suspension. Our results indicate that many-body hydrodynamic interactions have a significant effect for $\phi \gtrsim 0.3$.

In order to measure the self-mobility (rather than the more complicated collective dynamic properties) light-scattering measurements had to be made at values of the scattering vector much greater than those at which significant oscillations occur in the structure factor (see section 2). This necessitated the use of relatively large particles (diameter $\sim 1.2\ \mu$m). In order to obtain reasonably transparent dispersions at high concentrations it was necessary to match the refractive index of the liquid (in fact a mixture of liquids) closely to that of the particles. Experimental details and some of the difficulties encountered in light-scattering measurements on this rather unusual system are discussed in section 3.

2. **Theory.** — The simplest quantity which can be measured by dynamic light scattering from a concentrated suspension is the wavevector-dependent effective diffusion coefficient $D_{\text{eff}}(K)$, determined from the initial slope or « first cumulant » of the measured photon correlation function [1, 5-7]. For a large number $N$ of identical spherical particles, this coefficient can be written [7, and references therein]

$$D_{\text{eff}}(K) = [NK^2 S(K)]^{-1} \sum_{i,j=1}^{N} \langle \mathbf{K}.\mathbf{D}_{ij}(\{\mathbf{R}_l\}).\mathbf{K}\, e^{i\mathbf{K}.\mathbf{R}_{ij}} \rangle ; \quad (1)$$

here $\mathbf{K}$ is the scattering vector (magnitude $K$), $S(K)$ the static structure factor, $\mathbf{R}_{ij}$ the vectorial separation between the centres of particles $i$ and $j$ and the angular brackets represent an (ensemble) thermal average over all possible particle configurations. Equation (1) is valid on a timescale long enough that it is meaningful to talk about diffusive (Brownian) motion in response to the rapidly fluctuating solvent forces, but over which the particle positions barely change [1, 7]. $\mathbf{D}_{ij}(\{\mathbf{R}_l\})/kT$ is thus the mobility tensor which describes the velocity response (on this same timescale) of particle $i$ to a force on particle $j$ and depends, in the general case, on the instantaneous spatial configuration $\{\mathbf{R}_l\}$ of all the particles; $kT$ is the thermal energy.

If measurements are made at large enough $K$ (as in our experiments, see section 4), many oscillations occur in $\exp(i\mathbf{K}.\mathbf{R}_{ij})$ for small changes in $\mathbf{R}_{ij}$ and only $i = j$ terms survive the average in equation (1); for the same reasons $S(K)$ assumes its high-$K$ value of 1 (well beyond any oscillations). Thus, in this high-$K$ limit, equation (1) simplifies to

$$D^{S}_{\text{eff}} \equiv \lim_{K\to\infty} D_{\text{eff}}(K) = \langle \mathbf{K}.\mathbf{D}_{11}(\{\mathbf{R}_l\}).\mathbf{K} \rangle / K^2 \quad (2)$$

where $\mathbf{D}_{11}/kT$ is now the short-time *self*-mobility referred to in section 1. We have dropped the explicit dependence of $D_{\text{eff}}$ on $K$ since it becomes $K$-independent in this limit (see eq. 4); however we have kept the subscript « eff » to avoid confusion with the *long-time* self or tracer diffusion coefficient which describes the motion of particles over macroscopic distances (many interparticle spacings).

Several authors [2, 3] have considered the form of $\mathbf{D}_{11}$. For a pair of particles Felderhof [3] obtained an expansion for $\mathbf{D}_{11}$ to order $(a/R_{12})^6$, where $a$ is the particle radius. Recently Mazur and co-workers [8-10] have considered a many-particle system (see also Kynch [11]). Their lowest-order terms are the same as Felderhof's two-particle results and the next term is a three-body contribution of order $(a/R)^7$ :

$$\frac{\mathbf{D}_{11}(\{\mathbf{R}_l\})}{D_0} = \mathbf{1} + \sum_{j\neq 1} \frac{15}{4}\left(\frac{a}{R_{1j}}\right)^4 \hat{\mathbf{r}}_{1j}\,\hat{\mathbf{r}}_{j1} - \sum_{j\neq 1} \frac{1}{16}\left(\frac{a}{R_{1j}}\right)^6 (17\,\mathbf{1} + 105\,\hat{\mathbf{r}}_{1j}\,\hat{\mathbf{r}}_{j1}) +$$

$$+ \sum_{\substack{j,k\neq 1 \\ j\neq k}} \frac{75}{16}\frac{a^7}{R_{1j}^2 R_{jk}^3 R_{k1}^2} \{[1 - 3(\hat{\mathbf{r}}_{1j}.\hat{\mathbf{r}}_{jk})^2][1 - 3(\hat{\mathbf{r}}_{jk}.\hat{\mathbf{r}}_{k1})^2]$$

$$+ 6(\hat{\mathbf{r}}_{1j}.\hat{\mathbf{r}}_{jk})^2 (\hat{\mathbf{r}}_{jk}.\hat{\mathbf{r}}_{k1})^2 - 6(\hat{\mathbf{r}}_{1j}.\hat{\mathbf{r}}_{jk})(\hat{\mathbf{r}}_{jk}.\hat{\mathbf{r}}_{k1})(\hat{\mathbf{r}}_{k1}.\hat{\mathbf{r}}_{1j})\}(\hat{\mathbf{r}}_{1j}\,\hat{\mathbf{r}}_{k1}) + \cdots; \quad (3)$$

here $D_0$ is the « free-particle » diffusion constant, $R_{jk} = |\mathbf{R}_{jk}|$, $\mathbf{1}$ is the unit dyadic and $\hat{\mathbf{r}}_{jk}$ is a unit vector pointing from the centre of particle $j$ to the centre of particle $k$. Substitution of the one- and two-particle terms of equation (3) into equation (2) leads, after some manipulation, to [3, 6, 7]

$$D^{S}_{\text{eff}} = D_0\left[1 - \frac{3\phi}{a^3}\int_0^\infty dR\, R^2\, g(R)\left(\frac{5}{4}\frac{a^4}{R^4} - \frac{9}{8}\frac{a^6}{R^6}\right)\right], \quad (4a)$$

where $g(R)$ is the radial distribution function of the particles and the volume fraction $\phi \equiv \frac{4}{3}\pi\rho a^3$, $\rho$ being the average number of particles per unit volume.

Batchelor [2] has emphasized that, even for two particles, the series expansion of equation (3) becomes inaccurate for small interparticle separations due to neglect of two-body terms of higher order in $a/R$. He points out that the two-particle problem has been solved exactly (though numerically rather than analytically). Thus equation (4*a*) can be written more exactly as

$$D^{S}_{\text{eff}} = D_0\left[1 - \frac{3\phi}{a^3}\int_0^\infty dR\, R^2\, g(R)\left(1 - \frac{A_{11}}{3} - \frac{2B_{11}}{3}\right)\right], \quad (4b)$$

where $A_{11}$ and $B_{11}$ are components of the self hydrodynamic tensor, dependent on $a/R$, which are defined and tabulated by Batchelor [2b].

3. **Experimental details.** — Spherical colloidal latex particles of polymethyl methacrylate (PMMA) of radius approximately 0.6 μm, stabilized by a polyhydroxystearic acid coating, were obtained from Professor R. H. Ottewill's group at Bristol University in the form of a « paste » in dodecane. A weighed sample of this paste was dried to determine the latex weight fraction. A separate weighed sample was washed and centrifuged down several times in n-hexane. After removing most of the supernatant hexane and weighing again, we added carbon disulphide carefully until a relatively clear suspension was formed. This choice of liquids was dictated by the requirements of refractive-index matching (see below) and particle stability. By assuming the densities of latex, hexane and $CS_2$ to be 1.19, 0.659 and 1.263 $\text{mg.cm}^{-3}$ respectively, the latex volume fraction of the sample was calculated to be $\phi = 0.21$. Note that this calculation assumes the latex particles to be homogeneous; if, for example, the polymer coating were « loosely-packed » this approach could underestimate $\phi$, a possibility considered further in section 5.3. Higher volume fractions were obtained subsequently by removal of clear supernatant after the particles had been centrifuged down.

Measurements of the angle of minimum deviation of a laser beam through corners of the sample cell (having square cross-section) yielded dispersion refractive indices (RI). In order to obtain clear enough samples for light scattering it was necessary to obtain a dispersion refractive index within about 0.003 of that of the latex. The latter was estimated to range from 1.512 at wavelength $\lambda = 647$ nm to 1.524 at $\lambda = 476$ nm. During the process of concentration, and also if the laser wavelength was changed (since the RIs of the PMMA and liquid mixture had different dependences on wavelength), it was sometimes necessary to add a few drops of either $CS_2$ (RI $\approx$ 1.63) or hexane (RI $\approx$ 1.37) to obtain a better index match (see below).

Photon correlation dynamic light-scattering (DLS) measurements were made using standard equipment. The krypton ion laser was operated on any of four lines : red 647 nm, yellow 568 nm, green 521 nm and blue 476 nm. The sample cell, of square 1 cm × 1 cm cross-section, was placed so that the scattering volume (of linear dimension $\sim$ 200 μm) was within 1 mm of both its entrance (front) face and exit (side) face (see Fig. 3). This configuration provides a short path in the sample for the incident beam and single-scattered light seen by the detector, thereby maximizing the single-scattered intensity. Since the light scattering by these large particles is strongly peaked in the forward direction, this configuration also minimizes the intensity of detected multiple scattering : typically it would require many scattering events for a photon initially deviated by a small angle to reach the detector. The scattering angle $\theta$ was varied only in the range $60° < \theta < 120°$, although the scattering vector **K** was also varied by changing the laser wavelength. Room temperature was controlled to 19.5 ± 0.5 °C. The correlator sample time was chosen so that the observed electric field correlation function spanned only about half of a decay time or less; in this time a particle diffuses a distance equal to about 1/10 of its radius or less. Effective diffusion coefficients were obtained from a second-order cumulant fit. For the very dilute sample mentioned in section 4 the normalized second cumulant was found to be 0.04 ± 0.04, in adequate agreement with the value, $\lesssim$ 0.01, expected for a polydispersity of less than 10 %. At higher concentrations the dominant contribution to the second cumulant comes from the effect of interparticle interactions [7] and values as large as 1 or more were found.

At each concentration the sample was shaken vigorously, placed in the photometer and allowed to stand for an hour or so for residual swirling motions to cease; all light-scattering measurements were made within the next 24 hrs. Within a few hours the effects of gravitational settling were evident. A layer of clear supernatant appeared at the top of the sample and a dense layer of particles at the bottom. The observation of Bragg spots in the light scattered by this bottom layer showed the particles to be in a polycrystalline « solid » arrangement. DLS measurements were always made in the middle of the disordered « fluid-like » region between these layers. It was a fortunate occurrence that dust particles, which were quite evident when the sample was first placed in the equipment, appeared to vacate this region within a few hours.

We encountered several other experimental difficulties in the study of these concentrated suspensions. The attenuation, due to scattering, of the laser beam on passage through 1 cm of the sample was measured at various concentrations and wavelengths; we define an attenuation length by $L \equiv -(\ln T)^{-1}$ cm, where $T$ is the ratio of transmitted to incident intensities. We found that, for samples with $L$ greater than about 1.5 cm (i.e. a relatively close match between latex and liquid refractive indices where scattering is low), $D_{\text{eff}}$ was sometimes significantly larger than for samples with lower $L$ values. This effect seemed particularly marked for the yellow krypton line. The reasons for this observation were not firmly established; it is possible that a subpopulation of smaller particles (e.g. colloidal sulphur from degradation of the $CS_2$ [12]) becomes important when the latex particles scatter weakly. However we found that, if $L$ was kept below about 1.5 cm by suitable adjustment of dispersion refractive index, consistent results could be obtained at all wavelengths (see Fig. 1).

In fact measurements were occasionally made with $L$ as small as 0.3 cm. With such a strong scatterer, multiple scattering must be considered. As mentioned above, the light scattered by these relatively large particles is strongly peaked in the forward direction so that the dominant multiple scattering is also in this direction. Its effect at large scattering angles (as in the present work) is to reduce the apparent diffusion coefficient $D_{\text{eff}}(K)$ and, for $L \approx 0.3$ cm, the study of scattering from parts of the sample further away from the exit and entrance windows did show evidence of such distortions. Nevertheless, by using the scattering geometry shown in figure 3, we found that measurements could be made at large scattering angles without incurring significant multiple-scattering errors even in strongly-scattering samples of these large spheres.

We also observed that the laser beam became expanded somewhat after passage through a concentrated sample due, presumably, to absorption causing local heating and « thermal lensing ». When a high incident intensity (a few hundred mW) was used, semi-log plots of correlation functions of light scattered from the centre of a weakly-scattering sample occasionally showed downward curvature caused, we assume, by particle motions induced by convection. However, with strongly-scattering samples (smaller $L$), lower laser intensities (some tens of mW) could be used and such distortions were not observed.

The particle size was measured in three ways.

Firstly the angular positions of the first two minima in plots of the angle-dependence of the time-averaged intensity scattered by a dilute sample were compared with theoretical Mie scattering predictions. This gave a radius $a = 0.59 \pm 0.01$ μm. Secondly a dilute sample of latex in $CS_2$ (whose viscosity was known accurately from the literature) was studied by DLS. The radius calculated from the measured diffusion constant was $a = 0.58 \pm 0.02$ μm. Finally the lattice spacing of the polycrystalline solid of a sample which had settled for several weeks under gravity was determined from the positions of the « powder » diffraction rings. In fact these rings were found to be non-circular having horizontal radii a few percent smaller than vertical radii indicating some gravitational distortion of the crystals. The assumption of a face-centred-cubic lattice gave an average spacing $d$ of the 111 planes of $d = 1.03$ μm; in turn this gives an average centre-to-centre particle separation of $\sqrt{3/2}\, d = 1.26$ μm, several percent greater than the particle diameter $\sim 1.17$ μm measured by other techniques (above). Several factors could contribute to the difference. For one thing, a distorted crystal cannot be close-packed. Furthermore, computer simulations of hard spheres show complete crystallization for $\phi \gtrsim 0.55$ [13] (compared to $\phi = 0.74$ for close packing). Rough measurements of the volume of the crystal phase (with knowledge of the weight of latex in the sample) yielded a crystal volume fraction of $\phi \approx 0.61$. If this crystal could be « compressed » to close-packing, the particle separation would be roughly $1.26 \times (0.61/0.74)^{1/3}$ μm $= 1.18$ μm, in good agreement with the diameter measured by other methods.

4. **Results.** — Figure 1 shows the scattering-vector dependence of the effective diffusion coefficients $D_{\text{eff}}(K)$ of three samples, a dilute sample ($\phi \lesssim 0.005$) in a $CS_2$-hexane mixture (bottom curve) and two more concentrated samples. In fact the reciprocal $D_{\text{eff}}^{-1}(K)$ is plotted to conform with previous work [14] on interacting particles, where the effect of $S(K)$ (in eq. 1) was sought. We note that measurements made at different wavelengths superimpose quite well and that $D_{\text{eff}}(K)$ decreases with increasing concentration in accordance with the expectation that diffusion should be increasingly hindered.

The oscillations apparent in the data for the dilute sample are surprising at first sight since at this concentration interparticle interactions can be neglected and we expect $S(K) = 1$ and $D_{\text{eff}}(K) \approx D_0$ (eq. 1 with $\mathbf{D}_{ij} = \mathbf{1}\, D_0\, \delta_{ij}$) for all $K$. For the following reasons we believe they are due to polydispersity. The average intensity scattered at angle $\theta$ by a particle of radius $\approx 0.6$ μm exhibits about 5 minima as $\theta$ increases from 0 to 180°. The angular positions of these minima depend on particle size. Therefore, as the scattering angle or vector is changed, dynamic light scattering effectively samples different aspects of the particle size distribution of a polydisperse suspension; thus the apparent « free-particle » diffusion coefficient also shows an angle-dependence. It

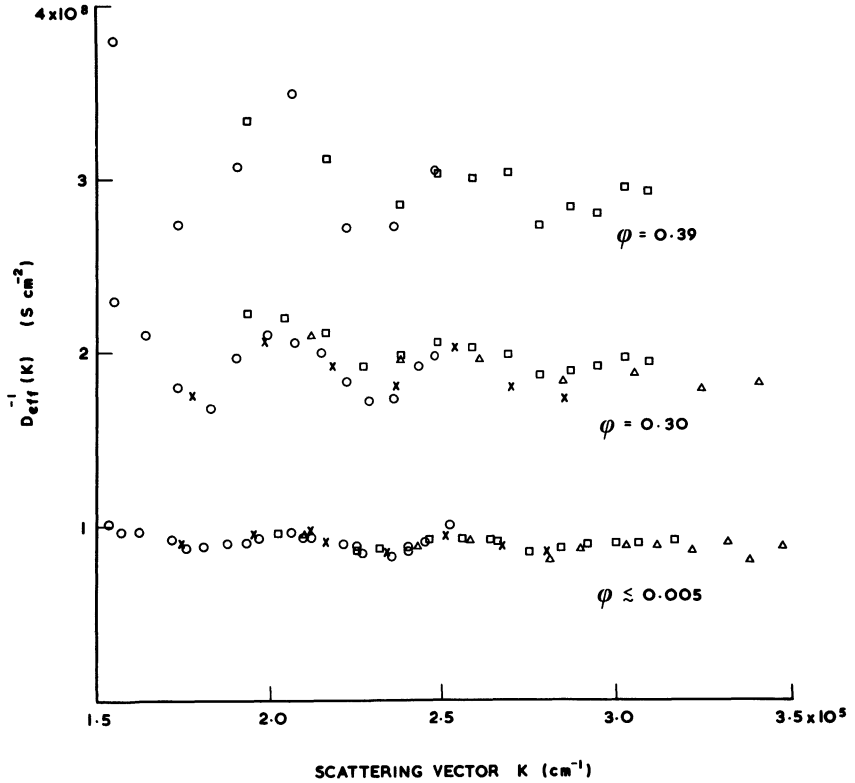


Fig. 1. — Reciprocal effective diffusion coefficients $D_{\text{eff}}^{-1}(K)$ as a function of scattering vector $K$ for three samples at volume fractions $\phi$ indicated. Measurements were made at four laser wavelengths : O-red, X-yellow, □-green, △-blue.

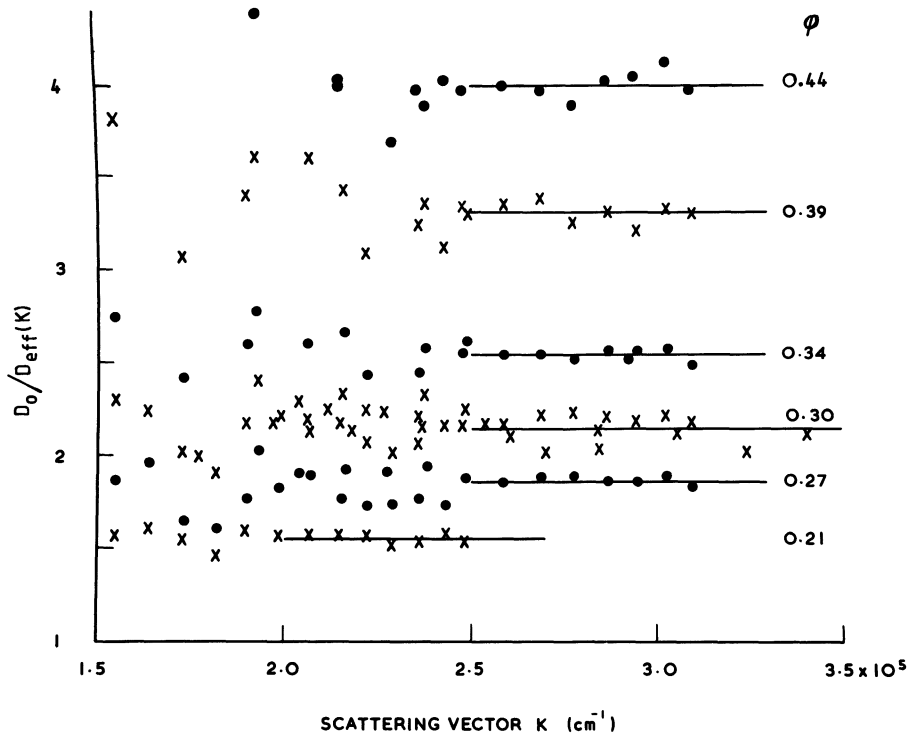


Fig. 2. — Reciprocal normalised effective diffusion coefficients $D_0/D_{eff}(K)$ as a function of scattering vector at volume fractions $\phi$ indicated. Measurements made at different wavelengths are not distinguished. Symbols ● and X are alternated with changing concentration to avoid confusion.

is probable that this effect can be exploited as a probe of polydispersity; this will be discussed elsewhere [15]. Here it suffices to say that curves of the type shown in figure 1 (for $\phi \approx 0$) can be obtained from a theoretical model for polydispersities of less than 0.1 (standard deviation/mean particle size).

In order to minimize this polydispersity effect, an estimated solid line (not shown in figure 1) was drawn through the dilute sample data. This provided an averaged ($K$-dependent) free-particle diffusion coefficient $D_0(K)$. The data for $D_{eff}^{-1}(K)$ obtained at higher concentrations were then multiplied by the appropriate value of $D_0(K)$ to provide estimates of $D_0/D_{eff}(K)$. The results of this operation are plotted in figure 2 where data for all the concentrated samples are shown; we see that, for $K \gtrsim 2.5 \times 10^5$ cm$^{-1}$, the oscillations are, within experimental error, removed. The fact that these normalized high-$K$ data are essentially independent of $K$ provides confirmation that off-diagonal ($i \neq j$) terms in equation (1) are negligible so that $D_{eff}(K)$ can confidently be interpreted as the single-particle mobility $D_{eff}^S$ of equation (2). For $K \lesssim 2.5 \times 10^5$ cm$^{-1}$, some oscillations are evident in the data, especially at high concentrations. The maximum in these data for $K \approx 2.0 \times 10^5$ cm$^{-1}$ coincides roughly with the expected 4th maximum in $S(K)$ for hard spheres of radius 0.59 μm.

By averaging the high-$K$ data (the solid lines in figure 2) we get estimates of $D_{eff}^S/D_0$ which are plotted as a function of volume fraction in figure 3. The error

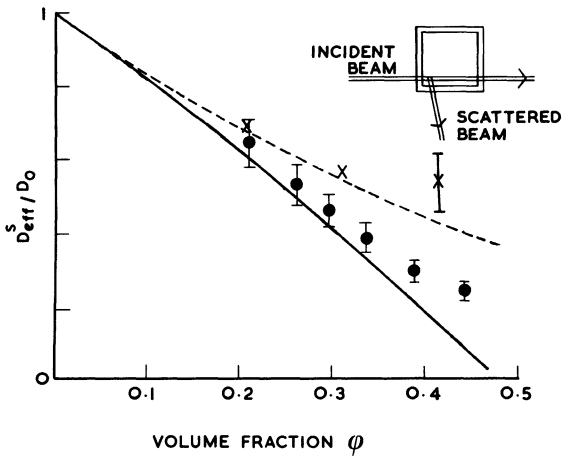


Fig. 3. — Upper right : Schematic of position of scattering volume in sample cell. Lower left : Data points ● are measured short-time self-diffusion coefficients $D_{eff}^S$ (relative to free-particle diffusion constant $D_0$) as a function of volume fraction. Solid line is « two-particle theory », the numerical evaluation of equation (4) with the « exact » hard-sphere $g(R)$ (see text). Dashed line is equation (8), the $O(\phi^2)$ density expansion which includes three-particle effects. The crosses X are discussed in the text.

bars are taken as ± 10 %, rather larger than implied by figure 2, in an attempt to include possible systematic errors arising from the experimental difficulties discussed in section 3.

5. **Discussion.** — 5.1 EVALUATION OF THE THEORETICAL EXPRESSIONS. — Numerical evaluation of equation (2) can be approached in several ways. Firstly, one can calculate a « density expansion » of $D^S_{eff}$ in powers of the volume fraction $\phi$. Clearly, the $\phi^0$ contribution comes from substituting the first term in equation (3) into equation (2), giving $D^S_{eff} = D_0$. The $\phi^1$ contribution is obtained by using in equation (4*a*) the lowest-order approximation for $g(R)$ which, for hard spheres, is

$$g(R) = 0 \quad \text{for} \quad R < 2a$$
$$g(R) = 1 \quad \text{for} \quad R > 2a. \tag{5}$$

This leads to Felderhof's well known result [3]

$$D^S_{eff} = D_0(1 - 1.73\,\phi + \cdots). \tag{6}$$

There are two contributions of order $\phi^2$. The first is a two-body term which comes from using in equation (4*a*) the $\phi^1$ term in $g(R)$ for hard spheres [16] (i.e. the next-order correction to eq. 5). This can be evaluated analytically to give [10]

$$D^S_{eff} = D_0(1 - 1.73\,\phi - 0.93\,\phi^2 + \cdots) \quad \text{(two-particle)}. \tag{7}$$

The second $\phi^2$ term comes from substitution of the three-particle term in equation (3) into equation (2) and averaging over the lowest-order three-body spatial distribution function (the three-body analogue of eq. 5). This contribution has recently been evaluated numerically by Beenakker and Mazur [10] with the result

$$D^S_{eff} = D_0(1 - 1.73\,\phi + 0.88\,\phi^2 + \cdots) \quad \text{(two- and three-particle)}. \tag{8}$$

We are currently investigating an alternative approach [17] to the evaluation of equations (2) and (3) using expressions for $g(R)$ and its three-body analogue *valid to all orders in* $\phi$. To this end we used the method of Verlet and Weis [18] to compute $g(R)$ for hard spheres; this method modifies the Percus-Yevick hard-sphere result to bring it into agreement with computer simulations and therefore provides the best approximation to an exact hard-sphere $g(R)$ currently available. The resulting integral (eq. 4*a*) for the two-body contribution was evaluated numerically. Since no accurate analytic approximation exists for the three-body spatial distribution function we are using computer-generated (Monte-Carlo) configurations of hard spheres to perform the spatial average.

In figure 3 the lower (solid) line is the result of evaluating the one and two-body terms in equations (2) and (3) using the Verlet-Weis $g(R)$ (see above). For $\phi \lesssim 0.15$ this agrees, as it should, quite well with the (two-particle) result of equation (7) (not plotted in Fig. 3); even at $\phi = 0.4$ the $O(\phi^2)$ density expansion of equation (7) is lower than the « exact $g(R)$ » two-particle result by only about 20 %. The upper (dashed) line in figure 3 is equation (8), the $O(\phi^2)$ density expansion which includes three-body effects. The crosses are the results of the Monte-Carlo calculations discussed above. Again there is surprisingly close agreement between the density expansion and the « exact $g(R)$ » evaluations. Reasons for the rather large error on the Monte-Carlo calculation at $\phi = 0.42$ will be discussed elsewhere [17].

It should be emphasized that neither of these approaches provides a complete theory. Even to order $\phi^2$, the first approach neglects two- and three-particle terms in the expansion of equation (3) of higher order than $(a/R)^7$. While it does evaluate equations (2) and (3) to all orders in $\phi$, the second approach also neglects two-, three- and many-particle terms of higher order than $(a/R)^7$. We note that, by use of the Verlet-Weis $g(R)$ and Batchelor's approach to the hydrodynamics (eq. 4*b*), it is, in principle, possible to calculate « exactly » two-body contributions to $D^S_{eff}$ valid to all orders in both $a/R$ and $\phi$. Due to the relative inaccessibility of complete hydrodynamic data and the conceptual simplicity of the series expansion approach we have not done this. However we point out that the difference between the quantities in round brackets in equations (4*b*) and (4*a*) is *positive for all values of* $a/R$. To be more specific, calculations using Batchelor's tabulations [2*b*] show that, at $R/a = 2$ (i.e. touching spheres), $1 - (A_{11}/3) - (2B_{11}/3) = 0.148$ and $(5a^4/4R^4) - (9a^6/8R^6) = 0.065$; at $R/a = 2.1$ the values are 0.072 and 0.051 respectively; and for $R/a > 3$ the values are essentially the same. We conclude, therefore, that, since $g(R) \geqslant 0$, the evaluation of the exact equation (4*b*) will lead to theoretical predictions which lie *below* the solid line in figure 3 (the evaluation of eq. 4*a*), but probably by a relatively small amount. For example, to first-order in $\phi$, equation (4*b*) leads to [2b]

$$D^S_{eff} = D_0(1 - 1.83\,\phi),$$

a value smaller, but not by much, than that of equation (6).

5.2 COMPARISON OF THEORY AND EXPERIMENT. — First we note that the lowest volume fraction at which measurements were made, $\phi \approx 0.2$, probably represents about the highest volume fraction at which equation (8), the $O(\phi^2)$ density expansion of Beenakker and Mazur, is valid. We see that the data point in figure 3 at $\phi \approx 0.2$ does indeed lie nearer to the two- and three-particle prediction of equation (8) (the dashed line) than to the two-particle prediction (the solid line). However the (possibly generous) error estimate spans both theoretical predictions. There is a clear need for very precise measurements at $\phi < 0.2$.

For $\phi > 0.35$, the experimental points lie above the two-particle theoretical prediction by an amount

significantly greater than the estimated experimental error. In view of the considerations of the last paragraph of section 5.1, *this observation points unambiguously to the invalidity of assuming pairwise additivity of hydrodynamic interactions in concentrated particle suspensions.*

However we also see in figure 3 a significant difference at high $\phi$ between experiment and theory incorporating just two and three-body hydrodynamics. At these high volume fractions many-particle clusters become as probable as those of two or three particles. Thus a possible interpretation of our results is that, at high concentrations, the full theory would lead to a density expansion for $D_{\text{eff}}^{S}$, with terms of oscillating sign, which converges only slowly with increasing powers of $\phi$. Unless this expansion can be resummed in some way, the outlook for a full understanding of short-time self diffusion (and, presumably, of more complicated hydrodynamic properties) of concentrated particle suspensions is somewhat discouraging.

5.3 GENERAL COMMENTS. — Throughout this paper we have assumed that the polymer-coated particles, suspended in a mixture of two liquids, can reasonably be regarded as « hard spheres » in a homogeneous liquid continuum. These assumptions are worth further brief comment.

Firstly we mention that, at the highest volume fraction studied, $\phi \approx 0.44$, occasional « Bragg spots » were observed, particularly in the main diffraction ring. It thus appears that the sample contained small regions of solid crystalline phase in co-existence with the fluid-like phase. Such co-existing phases have been observed in other colloidal systems [19] and are well established in hard-sphere computer experiments [13] which predict the onset of the phase transition to occur at $\phi \approx 0.49$. This difference between observed and predicted phase-transition concentrations is probably associated with the structure of the polymer coatings of the particles. As discussed in section 3, if this coating is loosely-packed, the volume fraction will be underestimated by our calculation procedure. Furthermore, the inter-particle interaction cannot be truly « hard-sphere » and the « effective hard-sphere volume fraction » could be significantly larger than the calculated « bare » value. Note that if the data points in figure 3 were all moved a few percent to the right to allow for this, marginally better agreement between experiment and the three-particle theory would be found.

Secondly, we have, for simplicity, neglected possible complications caused by preferential solvation of the particles and « ordering » of the liquids at the particle/polymer surfaces.

6. **Conclusion.** — Measurements of the conceptually-simple short-time self diffusion coefficients of particles in liquid suspension show that hydrodynamic interactions cannot be assumed to be pairwise-additive at high concentrations.

**Acknowledgments.** — We are extremely grateful to Professor R. H. Ottewill for providing the PMMA spheres and to him and Dr. D. J. Cebula for early investigation of their dispersion properties in liquid mixtures. We thank Dr. R. J. A. Tough, Dr. R. B. Jones, Professor H. N. W. Lekkerkerker and Professor P. Mazur for valuable discussions, the latter for sending preprints of his work on many-particle hydrodynamic interactions, and the referees for several important suggestions.

*Note added in proof.* — Glendinning and Russel (*J. Colloid Interface Sci.* **89** (1982) 124) have recently evaluated equation (4*b*) using exact (numerical) data for $D_{11}$. As we conjectured in section 5.1, their results lie slightly below the solid line in figure 3 (the evaluation of equation (4*a*)).

## References

[1] For a review of light-scattering studies of suspensions of interacting particles see PUSEY, P. N., TOUGH, R. J. A., in *Dynamic light scattering and velocimetry : Applications of photon correlation spectroscopy*, Ed. R. Pecora (Plenum, New York, in press).

[2] BATCHELOR, G. K., *J. Fluid. Mech.* **52** (1972) 245 ; **74** (1976) 1.

[3] FELDERHOF, B. U., *Physica* **89A** (1977) 373 ; *J. Phys. A : Math. Nucl. Gen.* **11** (1978) 929.

[4] KOPS-WERKHOVEN, M. M., FIJNAUT, H. M., *J. Chem. Phys.* **74** (1981) 1618.

[5] RUSSEL, W. B., GLENDINNING, A. B., *J. Chem. Phys.* **74** (1981) 948.

[6] FIJNAUT, H. M., *J. Chem. Phys.* **74** (1981) 6857.

[7] PUSEY, P. N., TOUGH, R. J. A., *J. Phys. A : Math. Nucl. Gen.* **15** (1982) 1291.

[8] MAZUR, P., *Physica* **110A** (1982) 128.

[9] MAZUR, P., VAN SAARLOOS, W., *Physica* **115A** (1982) 21.

[10] BEENAKKER, C. W. J., MAZUR, P., *Phys. Lett. A* **91** (1982) 290.

[11] KYNCH, G. J., *J. Fluid. Mech.* **5** (1959) 193.

[12] OTTEWILL, R. H., private communication.

[13] ALDER, B. J., HOOVER, W. G., YOUNG, D. A., *J. Chem. Phys.* **49** (1968) 3688.

[14] For example, BROWN, J. C., PUSEY, P. N., GOODWIN, J. W., OTTEWILL, R. H., *J. Phys. A : Math. Nucl. Gen.* **8** (1975) 664.

[15] PUSEY, P. N., VAN MEGEN, W., to be published.

[16] KIRKWOOD, J. G., *J. Chem. Phys.* **3** (1935) 300.

[17] VAN MEGEN, W., SNOOK, I. K., PUSEY, P. N., to be published.

[18] VERLET, L., WEIS, J. J., *Phys. Rev. A* **5** (1972) 939.

[19] HACHISU, S., KOBAYASHI, Y., KOSE, A., *J. Colloid Interface Sci.* **42** (1973) 342.